

## Accepted Article

**Title:** A Novel Hexanuclear Cd-MOF Exhibiting Dual Mechanisms-triggering Fluorescence Quenching Response toward Fe<sup>3+</sup> Ions in DMF

**Authors:** Ying-Hui Zhang, Long-Sheng Li, Xi Wang, Yan-Yuan Jia, Shi-Xian Xu, and Mei-Hui Yu

This manuscript has been accepted after peer review and appears as an Accepted Article online prior to editing, proofing, and formal publication of the final Version of Record (VoR). This work is currently citable by using the Digital Object Identifier (DOI) given below. The VoR will be published online in Early View as soon as possible and may be different to this Accepted Article as a result of editing. Readers should obtain the VoR from the journal website shown below when it is published to ensure accuracy of information. The authors are responsible for the content of this Accepted Article.

**To be cited as:** *Eur. J. Inorg. Chem.* 10.1002/ejic.201701290

**Link to VoR:** <http://dx.doi.org/10.1002/ejic.201701290>

# A Novel Hexanuclear Cd-MOF Exhibiting Dual Mechanisms-triggering Fluorescence Quenching Response toward Fe<sup>3+</sup> Ions in DMF

Long-Sheng Li,<sup>[a]</sup> Xi Wang,<sup>[b]</sup> Yan-Yuan Jia,<sup>[a]</sup> Shi-Xian Xu,<sup>[b]</sup> Mei-Hui Yu,<sup>[b]</sup> Ying-Hui Zhang,<sup>\*[b]</sup>

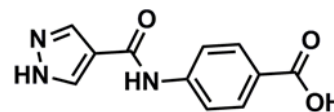
**Abstract:** A novel hexanuclear Cd(II) metal-organic framework (1) based on 4-(1H-pyrazole-4-carboxamido) benzoic acid (H<sub>2</sub>L) has been synthesized, featuring a three dimensional microporous framework. Notably, 1 shows a unique fluorescence quenching response toward Fe<sup>3+</sup> with high selectivity and sensitivity (Stern-Volmer constant  $K_{SV} = 2.07 \times 10^4 \text{ M}^{-1}$ ), attributable to the coaction of absorption competition and energy transfer (ET) mechanism. Further spectral analysis indicates that energy transfer mechanism contribute dominantly to the fluorescent quenching of 1.

## Introduction

Metal Organic Frameworks (MOFs) are constructed through ordered assembly of organic ligands and metal ions or clusters.<sup>1</sup> As a new class of inorganic-organic hybrid crystalline materials with tailorable topologies, MOFs have promising applications in many fields, including gas storage and separation,<sup>2</sup> catalysis,<sup>3</sup> drug delivery,<sup>4</sup> proton conduction,<sup>5</sup> chemical sensing,<sup>6</sup> and so on. Recently, increasing attention has been paid on the fluorescent response behaviors of MOFs toward guest species such as organic molecules and metal ions,<sup>7,8,9</sup> which favors the development of new kinds of fluorescent materials as well as new spectral analysis method. In general, the fluorescent response of MOFs may be triggered by many factors, including the collapse of the framework, ion-exchange process, absorption competition and energy transfer.<sup>10</sup> It's reasonable to hypothesis that the coaction of several factors would results in much sensitive fluorescence response, which, however, are confused due to difficult quantitative identification of the contribution from different effects.

As an essential transition metal involved in some biological processes,<sup>11,12</sup> It has been clearly demonstrated that the deficiency or overloading of iron will bring about various biological disorders, including hepatic cirrhosis, endotoxemia, hereditary hemochromatosis, and so on.<sup>13</sup> Therefore, various MOFs featuring fluorescent response toward Fe<sup>3+</sup> were developed and investigated in their response mechanism. Yan and coworkers reported an excellent fluorescent probe for Fe<sup>3+</sup> based on cation exchange mechanism.<sup>11b</sup> Our group has also

constructed some MOFs for selective detection of Fe<sup>3+</sup> based on ET mechanism or absorption competition mechanism.<sup>10e,10f</sup> However the MOFs exhibit fluorescent response toward iron ion triggered by multi-mechanism were less reported, and particularly, the strategy to quantitatively distinguish the contribution of different factors co-acting is scarcely investigated. In this work, we reported a Cd-MOF, namely {[Cd<sub>3</sub>(L<sup>2-</sup>)<sub>3</sub>(H<sub>2</sub>O)]·(DMF)·(H<sub>2</sub>O)}<sub>n</sub> (1) (H<sub>2</sub>L: 4-(1H-pyrazole-4-carboxamido) benzoic acid ligand, see Scheme 1), featuring highly selective and sensitive fluorescent quenching response toward Fe<sup>3+</sup> in DMF solution (Stern-Volmer constant  $K_{SV} = 2.07 \times 10^4 \text{ M}^{-1}$ ), which was ascribed to the coaction of absorption competition and ET mechanism based on spectral analyses. Furthermore, we develop a convenient and reliable method to assess the contribution from these two mechanisms.



Scheme 1 4-(1H-pyrazole-4-carboxamido) benzoic acid (H<sub>2</sub>L)

## Results and Discussion

### Crystal Structure of 1

Single-crystal X-ray diffraction analysis reveals that compound 1 crystallizes in the triclinic system with *P*-1 space group. The asymmetric unit consists of three crystallographically independent Cd (II) ions, three crystallographically independent L<sup>2-</sup> ligands, one coordinated water molecules, one lattice water and one lattice DMF guest. As illustrated in Fig. S1, Cd1 is five-coordinated by three N donors from three pyrazole rings of different L<sup>2-</sup> and two O atoms from other two L<sup>2-</sup>, forming a distort coordination configuration between tetragonal pyramid and trigonal bipyramid with a  $\tau$  value of 0.58;<sup>14</sup> Cd2 ion is coordinated by four chelating O atoms from two carboxylate groups of two L<sup>2-</sup> ligands, one water oxygen atom and one pyrazole N atoms, leading to a distorted octahedral geometry; Cd3 centers inside a distorted tetragonal pyramid geometry ( $\tau = 0.07$ )<sup>14</sup> surrounded by two chelating carboxylate oxygen atoms, two pyrazole N atoms of different L<sup>2-</sup> ligands, and one water molecule. These three kinds of Cd ions are bridged by carboxylate and pyrazole ring to form a linear trinuclear cluster. Meanwhile, two neighboring trinuclear clusters are double interlinked by two pyrazole ring to generate a hexanuclear Cd (II) cluster. For three kinds of L<sup>2-</sup>, there are two kinds of coordination modes observed for carboxylate group, one is  $\mu_2\text{-O}_1\text{:O}_2$  mode (L1) and the other is  $\mu_3\text{-O}_1\text{:O}_1\text{:O}_2$  mode (L2 and L3), while pyrazole group adopts only

[a] Department of Chemistry, Nankai University, Tianjin 300071, China  
E-mail: zhangyhi@nankai.edu.cn.

[b] School of Materials Science and Engineering, National Institute for Advanced Materials, Tianjin Key Laboratory of Metal and Molecule-Based Material Chemistry, Nankai University, Tianjin 300350, China.

Supporting information for this article is given via a link at the end of the document.

one  $\mu_2$ -N<sub>1</sub>:N<sub>2</sub> mode. In addition, a hydrogen bonding interaction was observed between L2 and one lattice DMF molecule (Fig. S2).

In the *ac* plane, adjacent hexanuclear Cd(II) clusters are linked by L3 ligands through Cd1 and Cd2 atoms, to form one dimensional (1D) chain (Fig. 1a). Each chain interacts with two neighboring ones through hydrogen bonding between the acrylamide group of L3 and the carboxylate group of L1, leading to a two-dimensional (2D) sheet (Fig. 1b). Furthermore, the 2D layers are pillared by L2, giving a three dimensional (3D) non-interpenetrated framework. Meanwhile, L1 acts as lateral pillar to strengthen the 3D framework (Fig. 1c). Careful inspection of the 3D framework reveals a channel with a section area of 7.5 Å × 9.0 Å (Fig. S3), which results in a total accessible volume of 49.5% for **1** by using PLATON software after removing lattice DMF molecules. To better understand the structure of **1**, the topological structure was analyzed by simplifying the ligands as three-connected nodes (L1) and four-connected nodes (L2 and L3), and Cd(II) ions as 3-connected nodes (Cd2 and Cd3) and 5-connected nodes (Cd1), which gives a (3,3,4,5)-connected 4-nodal net for **1** with a Schläfli symbol of {4·8<sup>2</sup>}\_2 {4<sup>2</sup>·8<sup>4</sup>}\_2 {4<sup>2</sup>·8<sup>3</sup>}\_2 {8<sup>2</sup>·12} (Fig. 1d).

#### Powder X-ray Diffraction Analyses (PXRD) and Thermogravimetric Analyses (TGA)

Before the measurement of fluorescence properties, the phase purity and stability of compound **1** were investigated by PXRD and TGA, respectively. The experimental diffraction pattern of the as-synthesized **1** matches very well with the simulated one based on single crystal data (Fig. S4), testifying the high phase purity of the sample. Thermogravimetric analyses were performed at air atmosphere after immersing **1** in ethanol for 2 days. As shown in Fig. S5, the mass loss (~20%) occurring before 150 °C corresponds to the escape of free solvent molecules as well as coordinated water, and no further mass loss was observed before the decomposition of **1** starting from 350 °C, manifesting the good thermal stability of **1**.

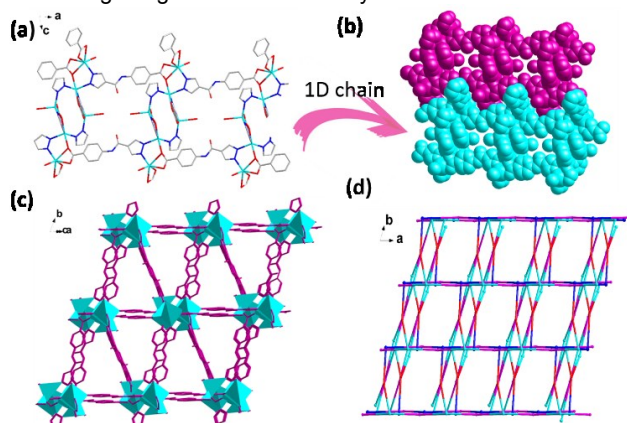


**Fig. 1** Single-crystal structure of **1**: (a) 1D chain formed by connecting hexanuclear Cd(II) cluster with L<sup>2</sup> in *ac* plane (color scheme: Cd, cyan; N, blue; O, red; C, 1/4 gray. H atoms are omitted for clarity); (b) 2D layer in space-filling mode formed by hydrogen bonding interaction between neighboring 1D chains; (c) The 3D framework of **1**. (d) The topological net of **1** with a Schläfli symbol of {4·8<sup>2</sup>}\_2 {4<sup>2</sup>·8<sup>4</sup>}\_2 {4<sup>2</sup>·8<sup>3</sup>}\_2 {8<sup>2</sup>·12}.

#### Fluorescence properties

The emission spectra of **1** and free ligand H<sub>2</sub>L were both measured (Fig. S6 and S7). As shown in Fig. S8, the fluorescence spectrum of **1** in DMF has the strongest emission at 347 nm ( $\lambda_{\text{ex}}=310$  nm), which is somewhat close to the 390 nm emission of free ligand in DMF solution ( $\lambda_{\text{ex}}=337$  nm), and thus is supposed to be ligand-dominated. Similar case is also observed for the solid sample (Fig. S7). The blue shifted emission observed for **1** relative to H<sub>2</sub>L can be rationally interpreted in terms of coordination interaction.

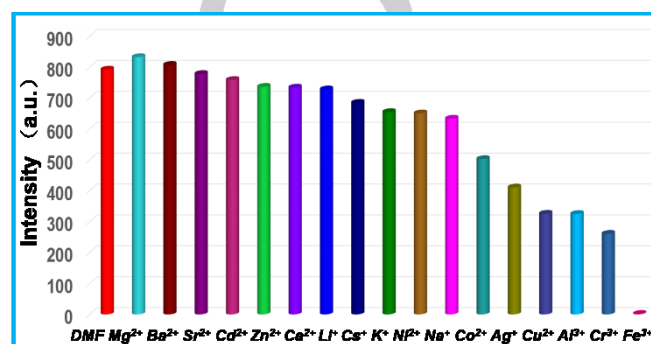


**Fig 2** The maximum emission intensities (at 347 nm) comparison among **1** suspension (in DMF,  $5 \times 10^{-4}$  M) and that upon the addition of various metal ions,  $\lambda_{\text{ex}} = 310$  nm.

#### Fluorescence response toward metal ions

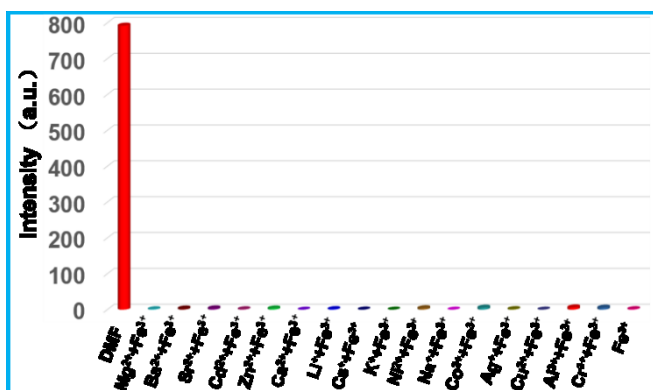
To explore the fluorescent respond of **1** toward various metal ions, 4 mg **1** was ground and dispersed in 3.8 mL dimethylformamide (DMF) to form suspension system after ultrasonication for 30 min. And then to the suspension system was added 0.2 mL DMF solution of M(NO<sub>3</sub>)<sub>x</sub> ( $1 \times 10^{-2}$  mol/L, M = Al<sup>3+</sup>, Li<sup>+</sup>, Na<sup>+</sup>, K<sup>+</sup>, Cs<sup>+</sup>, Mg<sup>2+</sup>, Ca<sup>2+</sup>, Sr<sup>2+</sup>, Ba<sup>2+</sup>, Ag<sup>+</sup>, Cr<sup>3+</sup>, Co<sup>2+</sup>, Ni<sup>2+</sup>, Zn<sup>2+</sup>, Cd<sup>2+</sup>, Cu<sup>2+</sup>, or Fe<sup>3+</sup>). The emission spectra of **1** suspension upon addition of different metal ions were collected in Fig. S8, and the emission intensities at 347 nm were compared in Fig. 2. It is clearly revealed that Fe<sup>3+</sup> drastically quenches the emission intensity of **1**, while other metal ions exert relatively negligible influence. This suggests the selective fluorescent response of **1** toward Fe<sup>3+</sup>.

In addition, the interference of other metal ions on the fluorescence response of **1** toward Fe<sup>3+</sup> was also explored. In a typical procedure, 0.2 mL DMF solution of Fe<sup>3+</sup> ( $1 \times 10^{-2}$  M) and 0.2 mL DMF solutions of another metal ions ( $1 \times 10^{-2}$  M) were added, sequentially and dropwise, into a 3.6 mL **1** suspension. The maximum emission intensity were recorded and compared with that of **1** as shown in Fig. 3, in which the great quenching effects of Fe<sup>3+</sup> on the fluorescence emission of **1** suspension was protruded even in the presence of other metal ions.

Above spectral analyses testified the selective fluorescence response of **1** toward Fe<sup>3+</sup>, which encouraged us to further evaluate the response sensitivity by spectral titration of **1** suspension with Fe<sup>3+</sup>. As shown in Fig. S9, the emission intensity of **1** suspension decreases gradually along with increasing addition of Fe<sup>3+</sup> with a total concentration growing from  $1 \times 10^{-7}$  to  $2.5 \times 10^{-4}$  M. The Stern-Volmer equation,  $I_0/I = 1 + K_{\text{sv}} [M]$ , was used to evaluate the quenching effect, where  $I_0$  and  $I$  stand for the

fluorescence intensity before and after the addition of metal ions, respectively,  $K_{SV}$  is the Stern-Volmer constant, and  $[M]$  is the concentration of  $Fe^{3+}$ . According to spectral titration data, the linear relationship between  $I_0/I$  and  $[M]$  was simulated in Fig 4, with a  $K_{SV}$  of about  $2.07 \times 10^4 M^{-1}$ . This  $K_{SV}$  value is comparable to that of some organic sensors for  $Fe^{3+}$ ,<sup>15</sup> which manifests the high response sensitivity of **1** toward  $Fe^{3+}$ .

Fig 3 The quenching effects of  $Fe^{3+}$  on the emission intensity of **1** suspension



in the presence of other metal ions,  $\lambda_{ex} = 310$

The recyclability of fluorescence materials is crucial for their practical application and thus was also investigated for **1** here. The recovery of **1** after fluorescence response is carried out by centrifuging the suspension and then washing the collected precipitate with DMF for three times. Similar PXRD pattern verifies the same crystal structure of the recovered **1** with that of as-synthesized one (Fig. S10). After repeating the response/recovery procedure for three times, **1** still exhibits highly sensitive response toward  $Fe^{3+}$  (Fig. S11), which unveils the good repeatability of **1** in fluorescence response toward  $Fe^{3+}$ .

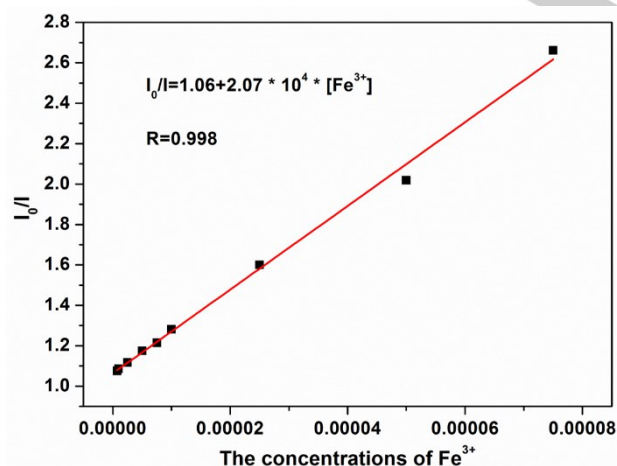


Fig 4 The Stern-Volmer plot predicted based on fluorescence spectral titration of **1** suspension with  $Fe^{3+}$ , where  $I_0$  and  $I$  stand for the emission intensity of **1** suspension before and after the addition of  $Fe^{3+}$  ion, respectively.

#### Fluorescence response mechanism analyses

In general, fluorescence emission quenching of MOFs may be triggered by many factors, including the decomposition of the

framework, cation exchange, absorption competition or energy transfer. In the following section, we tried to clarify the mechanism of the selective fluorescence response of **1** toward  $Fe^{3+}$ .

The influence of possible decomposition of framework can firstly be excluded as supposed by the similar PXRD pattern of the recovered **1** to that of as-synthesized one illustrated in Fig. S10. Moreover, inductive coupled plasma spectroscopy (ICP) experiment of recovered **1** reveals much higher content of Cd element relative to Fe (Table S4), suggesting negligible degree of cation exchange. Moreover, the good recyclability also strongly suggests the fluorescence quenching should be ascribed to other factors.

Considering the spectral properties of **1**, the action of absorption competition or energy transfer mechanism is of great possibility. To verify this assumption, the UV-Vis absorption spectra of metal ions solution were measured and compared with the fluorescence spectra of **1** suspension. As shown in Fig. 5,  $Fe^{3+}$  exhibits strong absorption in a wide range from 285 to 500 nm, originating from the d-d electron transition. This overlaps greatly both with the excitation (285-325 nm) and emission (340-500 nm) regions of **1**, and consequently may result in great quenching of the fluorescent emission of **1**. On contrary, no obvious absorption was observed in these two regions for other metal ions studied here, which is consistent with the little or negligible fluorescence response of **1** toward other metal cations. Based on above analyses, it is deduced convincingly that the coaction of absorption competition and energy transfer may account for the highly sensitive fluorescence response of **1** towards  $Fe^{3+}$ .

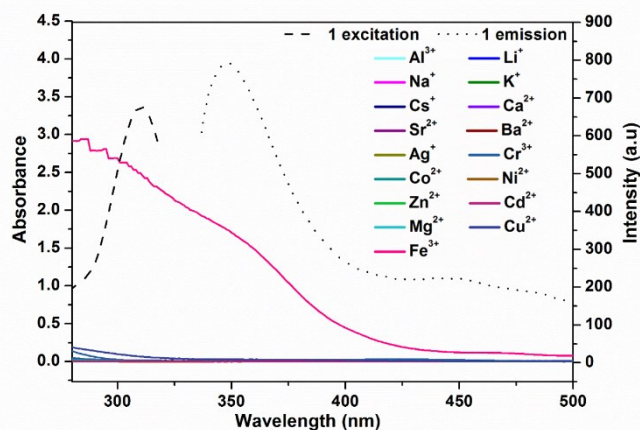


Fig 5 The absorption spectra of the DMF solutions of  $5 \times 10^{-4} M M(NO_3)_x$  (solid line,  $M = Al^{3+}, Li^+, Na^+, K^+, Cs^+, Ca^{2+}, Sr^{2+}, Ba^{2+}, Ag^+, Cr^{3+}, Co^{2+}, Ni^{2+}, Zn^{2+}, Cd^{2+}, Mg^{2+}, Cu^{2+}, Fe^{3+}$ ) and the excitation (dashed line) and emission profile (dotted line) of **1** dispersed in DMF (4 mg in 4 mL).

It's necessary to evaluate the contribution from these two mechanisms to the fluorescence quenching, respectively. Accordingly, a convenient and reliable experiment was performed to assess the contribution only from absorption competition as shown in Figure S12, where the  $Fe^{3+}$  ion was increasingly added into 4 mL DMF solution in the cuvette placed in the incident path before sample cell. This setting would

exclude the possible contribution from energy transfer to the fluorescence quenching and thus give a convincing assessment of the role of absorption competition. The simulation based on this experimental data with Stern-Volmer equation gives a slope of ca. 4800 (abbreviated as  $K'_{SV}$ ). By comparing  $K'_{SV}$  and  $K_{SV}$ , it is reliably concluded that the contribution from energy transfer mechanism is dominant.

## Conclusions

In summary, a novel hexanuclear Cd-MOF (**1**) was constructed with 4-(1H-Pyrazole-4-carboxamido) benzoic acid ligand. The good selectivity, high sensitivity (Stern-Volmer constant  $K_{SV} = 2.07 \times 10^4 \text{ M}^{-1}$ ) and repeatability of **1** in fluorescence response toward  $\text{Fe}^{3+}$ , based on absorption and fluorescence spectral analyses, were ascribed to the coaction of absorption competition and ET mechanism. Further spectral analysis indicates that ET contributes mainly to the fluorescence quenching of **1**.

## Experimental Section

### Materials and methods

All reagents and solvents used for synthesis were AR grade and used as received without further purification. 4-(1H-Pyrazole-4-carboxamido) benzoic acid (**H<sub>2</sub>L**) was synthesized according to the method reported earlier.<sup>16</sup> <sup>1</sup>H NMR spectra were recorded on a Varian Mercury Vx-300 spectrometer. Powder X-ray diffraction (PXRD) data were collected over a  $2\theta$  range from  $3^\circ$  to  $50^\circ$  on a Rigaku D/Max-2500 diffractometer using Cu radiation and a graphite monochromator at room temperature. Thermogravimetric (TG) analyses were carried out on a Rigaku PTC-10A TG-DTA analyzer with a heating rate of  $10^\circ\text{C min}^{-1}$  from ambient temperature to  $800^\circ\text{C}$  in air using an  $\text{Al}_2\text{O}_3$  crucible as reference. IR spectra were recorded on a TENSOR 37 (Bruker) FT-IR spectrometer with KBr pellets. UV/Vis absorption spectra were measured with a Hitachi U-3010 UV-Vis spectrophotometer (Hitachi, Japan). Fluorescence spectra were recorded at room temperature on a Hitachi F-4500 fluorescence spectrometer. Elemental analyses (C, H and N) were performed on a Perkin-Elmer analyzer. Inductively coupled plasma (ICP) analyses were carried out on a Perkin-Elmer Optima 3300 DV spectrometer.

### Synthesis of 4-(1H-Pyrazole-4-carboxamido) benzoic acid (**H<sub>2</sub>L**).

A mixture of 1H-pyrazole-4-carboxylic acid (30 mmol), freshly distilled thionyl chloride (60 mL) and two drops of dry DMF was heated to reflux for 12h at nitrogen atmosphere. Then excess thionyl chloride was removed by distillation under reduced pressure and the resultant crystalline powder of 1H-pyrazole-4-carbonyl chloride was collected. Subsequently, a mixture of 4-aminobenzoic acid (30 mmol), DMA (15 mL), and N,N-dimethyl-4-aminopyridine (0.001 mol) was stirred in a 250 mL flask, bubbled with nitrogen, and heated at  $80^\circ\text{C}$  for 30 min. The solution was then cooled to  $10^\circ\text{C}$  and then added with 30 mmol 1H-pyrazole-4-carbonyl chloride. This reaction mixture was heated slowly to  $40^\circ\text{C}$  and added with pyridine (60 ml). After 24 h the mixture was cooled to ambient temperature and poured into 5% hydrochloric acid. The resultant precipitate was filtered, washed with hot water three times and then dried in air. Yield based on 1H-pyrazole-4-carboxylic acid : 80%; <sup>1</sup>H

NMR (300 MHz, DMSO- $d_6$ ,  $\delta$ ppm): 10.5 (s, 1H, CONH), 8.23 (s, 2H, CH (pyrazole)), 7.91, 7.89, 7.84 and 7.81 (q, 4H, ArH) (see Fig. S13).

### Synthesis of $\{[\text{Cd}_3(\text{L}^2)_3(\text{H}_2\text{O})] \cdot (\text{DMF}) \cdot (\text{H}_2\text{O})\}_n$ (**1**).

To a mixture of 3 ml N,N-dimethylformamide (DMF) and 0.5 ml ethanol ( $\text{C}_2\text{H}_5\text{OH}$ ) in 20 ml Teflon-lined stainless steel autoclave,  $\text{CdCl}_2 \cdot 2.5\text{H}_2\text{O}$  (56 mg, 0.2 mmol) and  $\text{H}_2\text{L}$  (23.1 mg, 0.1 mmol) were dissolved. The autoclave was heated at  $150^\circ\text{C}$  for 2 days under autogenous pressure and then cooled slowly to room temperature at a rate of  $5^\circ\text{C/h}$  under ambient conditions. The resulting pale yellow crystals were collected and washed with DMF. The product yield was 60% estimated based on  $\text{H}_2\text{L}$ . Elemental analysis calc. for  $(\text{C}_{36}\text{H}_{32}\text{N}_{10}\text{O}_{12}\text{Cd}_3)$ : C, 38.16; H, 2.82; N, 12.36; found C, 38.32; H, 3.15; N, 13.14. FT-IR (KBr pellets,  $\text{cm}^{-1}$ ): 1659.14(s); 1600.83(s); 1543.35(s); 1504.05(s); 1389.40(s); 1311.81(m); 1175.89(m); 783.71(m); 660.17(m) (Fig. S14).

### Determination of Crystal Structure

The X-ray diffraction data was collected on a Rigaku SCX-mini diffractometer at 293 K with a Mo-K $\alpha$  radiation ( $\lambda = 0.71073 \text{ \AA}$ ) at scan mode. The structure was solved by direct methods and all non-hydrogen atoms were located from the trial structures and then refined anisotropically on  $F^2$  refined by full-matrix least-squares procedures using SHELXTL. All H atoms were refined isotropically with the isotropic vibration parameters related to the non-hydrogen atoms to which they are bonded. The guest molecules in **1** are disordered and could not be modeled properly, and so were removed by SQUEEZE in PLATON<sup>47</sup> (the results were appended in the CIF files). Detailed crystallographic data are summarized in Table S1 and some selected bond lengths and angles are listed in Tables S2 and S3. The crystallographic data of **1** has been deposited in CCDC (1549978) and can be obtained free of charge from the Cambridge Crystallographic Data Centre via [www.ccdc.cam.ac.uk/data\\_request/cif](http://www.ccdc.cam.ac.uk/data_request/cif).

## Acknowledgements

This work was financially supported by the NSFC (21371102, 21531005, and 21673120) and the NSF of Tianjin (15JCZDJC38800 and 16JCZDJC36900).

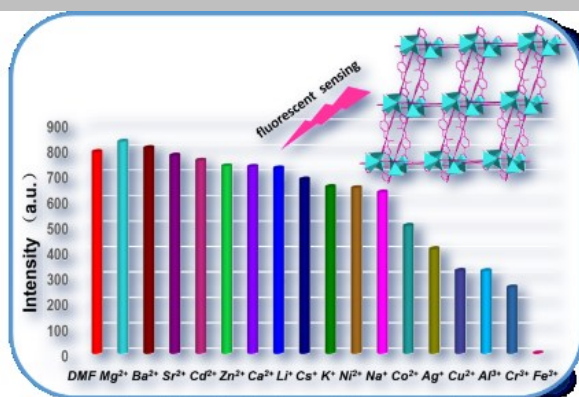
**Keywords:** Cd-MOF • Absorption competition • Energy transfer • Dual quenching mechanism • High sensitivity

- [1] a) J. A. Mason, T. M. McDonald, T.-H. Bae, J. E. Bachman, K. Sumida, J. J. Dutton, S. S. Kaye and J. R. Long, *J. Am. Chem. Soc.* **2015**, *137*, 4787-4803; b) H. Wu, J. Yang, Z.-M. Su, S. R. Batten and J.-F. Ma, *J. Am. Chem. Soc.* **2011**, *133*, 11406-11409; c) D. Bradshaw, A. Garai and J. Huo, *Chem. Soc. Rev.* **2012**, *41*, 2344-2381; d) O. M. Yaghi, *Nat. Mater.* **2007**, *6*, 92-93; e) Y.-Y. Jia, G.-J. Ren, A.-L. Li, L.-Z. Zhang, R. Feng, Y.-H. Zhang and X.-H. Bu, *Cryst. Growth Des.* **2016**, *16*, 5593-5597.
- [2] a) O. Benson, I. da Silva, S. P. Argent, R. Cabot, M. Savage, H. G. W. Godfrey, Y. Yan, S. F. Parker, P. Manuel, M. J. Lennox, T. Mitra, T. L. Easun, W. Lewis, A. J. Blake, E. Besley, S. Yang and M. Schröder, *J. Am. Chem. Soc.* **2016**, *138*, 14828-14831; b) X.-T. Liu, Y.-Y. Jia, Y.-H. Zhang, G.-J. Ren, R. Feng, S.-Y. Zhang, M. J. Zaworotko and X.-H. Bu, *Inorg. Chem. Front.* **2016**, *3*, 1510-1515; c) R. B. Getman, Y.-S. Bae, C. E. Wilmer and R. Q. Snurr, *Chem. Rev.* **2012**, *112*, 703-723; d) F. Moreau, I. da Silva, N. H. Al Smail, T. L. Easun, M. Savage, H. G. W.

- Godfrey, S. F. Parker, P. Manuel, S. Yang and M. Schröder, *Nat. Commun.* **2017**, *8*, 14085; e)
- [3] a) H. Xu, B. Zhai, C.-S. Cao and B. Zhao, *Inorg. Chem.* **2016**, *55*, 9671-9676; b) X. He, K. Fang, X.-H. Guo, J. Han, X.-P. Lu and M.-X. Li, *Dalton Trans.* **2015**, *44*, 13545-13549; c) M. Yoon, R. Srirambalaji and K. Kim, *Chem. Rev.* **2012**, *112*, 1196-1231; d) Z.-L. Wu, C.-H. Wang, B. Zhao, J. Dong, F. Lu, W.-H. Wang, W.-C. Wang, G.-J. Wu, J.-Z. Cui and P. Cheng, *Angew. Chem. Int. Ed.* **2016**, *128*, 5022-5026.
- [4] a) X. Zhu, J. Gu, Y. Wang, B. Li, Y. Li, W. Zhao and J. Shi, *Chem. Commun.* **2014**, *50*, 8779-8782; b) H. Wang, J. Xu, D.-S. Zhang, Q. Chen, R.-M. Wen, Z. Chang, X.-H. Bu, *Angew. Chem. Int. Ed.* **2015**, *54*, 5966-5970.
- [5] a) A.-L. Li, Q. Gao, J. Xu, X.-H. Bu, *Coord. Chem. Rev.* **2017**, *344*, 54-82; b) Y.-S. Wei, X.-P. Hu, Z. Han, X.-Y. Dong, S.-Q. Zang and T. C. W. Mak, *J. Am. Chem. Soc.* **2017**, *139*, 3505-3512.
- [6] a) C. Qiao, X. Qu, Q. Yang, Q. Wei, G. Xie, S. Chen and D. Yang, *Green Chem.* **2016**, *18*, 951-956; b) H. Xu, H.-C. Hu, C.-S. Cao and B. Zhao, *Inorg. Chem.* **2015**, *54*, 4585-4587; c) B. Chen, L. Wang, Y. Xiao, F. R. Fronczek, M. Xue, Y. Cui and G. Qian, *Angew. Chem. Int. Ed.* **2009**, *48*, 500-503; d) X.-J. Liu, Y.-H. Zhang, Z. Chang, A.-L. Li, D. Tian, Z.-Q. Yao, Y.-Y. Jia and X.-H. Bu, *Inorg. Chem.* **2016**, *55*, 7326-7328.
- [7] a) S.-G. Chen, Z.-Z. Shi, L. Qin, H.-L. Jia and H.-G. Zheng, *Cryst. Growth Des.* **2017**, *17*, 67-72; b) D. Curiel, M. Más-Montoya and G. Sánchez, *Coord. Chem. Rev.* **2015**, *284*, 19-66; c) M. Formica, V. Fusi, L. Giorgi and M. Micheloni, *Coord. Chem. Rev.* **2012**, *256*, 170-192; d) S. M. Ng and R. Narayanaswamy, *Anal. Bioanal. Chem.* **2006**, *386*, 1235-1244; e) Y. Wu, G.-P. Yang, Y. Zhao, W.-P. Wu, B. Liu and Y.-Y. Wang, *Dalton Trans.* **2015**, *44*, 3271-3277.
- [8] P. Mahata, S. K. Mondal, D. K. Singha and P. Majee, *Dalton Trans.* **2017**, *46*, 301-328.
- [9] a) Y.-P. Wu, G.-W. Xu, W.-W. Dong, J. Zhao, D.-S. Li, J. Zhang and X. Bu, *Inorg. Chem.* **2017**, *56*, 1402-1411; b) L.-J. Han, W. Yan, S.-G. Chen, Z.-Z. Shi and H.-G. Zheng, *Inorg. Chem.* **2017**, *56*, 2936-2940
- [10] a) Y.-T. Liang, G.-P. Yang, B. Liu, Y.-T. Yan, Z.-P. Xi and Y.-Y. Wang, *Dalton Trans.* **2015**, *44*, 13325-13330; b) C. A. Kent, B. P. Mehl, L. Ma, J. M. Papanikolas, T. J. Meyer and W. Lin, *J. Am. Chem. Soc.* **2010**, *132*, 12767-12769; c) Y. Li, H. Song, Q. Chen, K. Liu, F.-Y. Zhao, W.-J. Ruan and Z. Chang, *J. Mater. Chem. A* **2014**, *2*, 9469-9473; d) H.-N. Wang, S.-Q. Jiang, Q.-Y. Lu, Z.-Y. Zhou, S.-P. Zhuo, G.-G. Shan and Z.-M. Su, *RSC Adv.* **2015**, *5*, 48881-48884. e) L. Wang, Z.-Q. Yao, G.-J. Ren S.-D. Han, T.-L. Hu and X.-H. Bu *Inorg Chem Commun.* **2016**, *65*, 9-12.
- [11] a) Q. Tang, S. Liu, Y. Liu, J. Miao, S. Li, L. Zhang, Z. Shi and Z. Zheng, *Inorg. Chem.* **2013**, *52*, 2799-2801; b) C.-X. Yang, H.-B. Ren and X.-P. Yan, *Anal. Chem.* **2013**, *85*, 7441-7446; c) G.-G. Hou, Y. Liu, Q.-K. Liu, J.-P. Ma and Y.-B. Dong, *Chem. Commun.* **2011**, *47*, 10731-10733.
- [12] a) Z.-Q. Liang, C.-X. Wang, J.-X. Yang, H.-W. Gao, Y.-P. Tian, X.-T. Tao and M.-H. Jiang, *New J. Chem.* **2007**, *31*, 906-910; b) S. Dang, E. Ma, Z.-M. Sun and H. Zhang, *J. Mater. Chem.* **2012**, *22*, 16920-16926; c) K. Rurack and U. Resch-Genger, *Chem. Soc. Rev.* **2002**, *31*, 116-127.
- [13] a) J. L. Bricks, A. Kovalchuk, C. Trieflinger, M. Nofz, M. Büschel, A. I. Tolmachev, J. Daub and K. Rurack, *J. Am. Chem. Soc.* **2005**, *127*, 13522-13529; b) X.-Y. Xu and B. Yan, *ACS Appl. Mater. Interfaces.* **2015**, *7*, 721-729.
- [14] A. W. Addison, T. N. Rao, J. Reedijk, J. van Rijn and G. C. Verschoor, *J. Chem. Soc., Dalton Trans.* **1984**, *3*, 1349-1356.
- [15] S. K. Sahoo, D. Sharma, R. K. Bera, G. Crisponi and J. F. Callan, *Chem. Soc. Rev.* **2012**, *41*, 7195-7227.
- [16] J. J. Ferreira, J. G. de la Campa, A. E. Lozano and J. de Abajo, *J. Poly. Sci. A* **2005**, *43*, 5300-5311.
- [17] A. Spek, *J. Appl. Cryst.* **2003**, *36*, 7-13.

## FULL PAPER

A novel hexanuclear Cd-MOF was constructed with highly selective and sensitive fluorescent quenching response toward  $\text{Fe}^{3+}$ , attributable to the coaction of absorption competition and energy transfer mechanism.

**Key Topic\***

Long-Sheng Li, Xi Wang,  
Yan-Yuan Jia, Shi-Xian Xu,  
Mei-Hui Yu, Ying-Hui Zhang

**Page No. – Page No.**

**A Novel Hexanuclear  
Cd-MOF Exhibiting Dual  
Mechanism-Triggering  
Fluorescence Quenching  
Response toward  $\text{Fe}^{3+}$  Ions  
in DMF**